# Rpt6 Tail influences the Competition between Nas6 and Core Particle in Proteasome Assembly

Frances Shieh Li
Department of Molecular, Cellular and Developmental Biology
University of Colorado at Boulder
April 2nd, 2015

Dr. Soyeon Park, Thesis Advisor
Department of Molecular, Cellular, and Developmental Biology

Thesis Committee Members:
Dr. Christy Fillman, Honors Council Representative
Dr. Nancy Guild, MCDB Representative
Department of Molecular, Cellular, and Developmental Biology

Dr. Sabrina Spencer, Biochemistry Representative
Department of Chemistry and Biochemistry

## Abstract

The 26S proteasome is a molecular machine for regulated protein degradation in eukaryotes. In order to build a functional proteasome, proper assembly between the 19-subunit regulatory particle (RP) and 28-subunit core particle (CP) is very crucial. RP assembly relies on four evolutionarily conserved chaperones: Nas6, Rpn14, Hsm3, and Nas2 (1-4). These chaperones bind to RP and prevent their premature interaction with CP. However, it is unknown what controls the switch between chaperone-RP state and CP-RP (proteasome holoenzyme) state. In this project, I focus on the Nas6 chaperone to understand how Nas6 and CP compete for RP to achieve successful assembly of the proteasome in *Saccharomyces cerevisiae*. I also examine potential factors that can further shift the competition between Nas6 and CP to probe how cells coordinate proteasome assembly with metabolic states in cell.

## Introduction

Our cells employ numerous processes to maintain protein homeostasis and cell viability. One of the most crucial process is the ability for our cells to eliminate proteins. Whether it is misfolded proteins or transcription factors that do not need to be present anymore, the task of degrading these proteins falls upon a complex protein machinery called the 26S proteasome in eukaryotes. Substrates of the 26S proteasomes are involved in cellular processes like cell cycle and transcription (5, 6). Impairment in proteasome function results in deregulation of these fundamental cellular pathways and also contributes to pathogenic conditions such as Alzheimer's and Parkinson's syndrome. To achieve degradation in a regulated and timely manner, the proteasome recognizes and degrades proteins that are ubiquitinated (7), meaning proteins that are conjugated to ubiquitins (usually to a chain of ubiquitins). Therefore, the degradation of proteins by the proteasome is very precise and regulated.

### Structure of the 26S proteasome and assembly of the RP-CP interface

The 26S proteasome is composed of 33 different subunits, and it is divided into two complexes: the 20S core particle (CP) and the 19S regulatory particle (RP). The 26S proteasome is an ATP-dependent protease. ATP binding and hydrolysis are essential when the RP recognizes ubiquitinated proteins, unfolds and translocates them into the CP, where degradation occurs. The proteolytic CP has a barrel-shaped structure that is composed of four stacks of hetero-heptameric ring in the order of: $\alpha_{1-7}$–$\beta_{1-7}$–$\beta_{1-7}$–$\alpha_{1-7}$ (4). CP contains the proteolytic activities of the 26S proteasome and the only way to access it is through the opening of the 'gate', which is formed by the N-terminus of $\alpha 1$–$\alpha 7$ (8). Later, I will discuss what allows the opening of the 'gate'.

The RP is divided in to lid and base sub-complexes. An important aspect of my project

is the base and its six ATPase subunits, referred to as Rpt proteins, which are arranged into a heter-hexameric 'Rpt ring'. The Rpt ring sits directly on top of the CP and provides a major affinity for RP-CP interaction. The lid act as a clamp from the side, further stabilizing the RP-CP interface (9). The formation of proper RP-CP interface is very important in that it is the step before having a functional proteasome. Increased RP-CP assembly has been shown recently as a major mechanism for increased proteasome activities when proteolytic demands rise in cell (10, 11).

The six ATPase subunits (Rpt1–Rpt6) of the base governs the RP-CP interaction of the proteasome. At the RP-CP interface, a hetero-hexameric Rpt ring aligns with the hetero-heptameric $\alpha$ ring of the CP (12). The $\alpha$ ring has seven pockets formed between the two neighboring $\alpha$ subunits. The short C-terminal tail of the Rpt inserts into the individual $\alpha$ pocket and forms salt-bridge with the conserved lysine inside the $\alpha$ pocket to form the RP-CP interaction (13). C-termini of all six Rpts are evolutionarily conserved. Besides serving to maintain RP-CP interaction, three Rpt proteins (Rpt2, Rpt3, and Rpt5) contain the HbYX-motif (hydrophobic-tryosine-any amino acid) in their C-termini (8). The docking of HbYX tails activates the proteasome by opening the CP gate for the entry of the substrates for degradation.

**The involvement of RP chaperones in RP-CP formation**

Four dedicated and conserved chaperons assist in RP assembly: Nas6, Nas2, Hsm3, and Rpn14 (1-4). Each chaperone binds to specific Rpt proteins in their C-domain as follows: Nas6-Rpt3, Rpn14-Rpt6, Hsm3-Rpt1, and Nas2-Rpt5 (2, 14-17). Although phylogenetically distinct, these chaperones promote Rpt ring assembly by antagonizing premature Rpt tail-CP interaction. Specifically, Nas6 and CP compete for Rpt3 tail. In the current model, Nas6 wins the competition at early stage assembly; Na6 binding to Rpt3 C-domain prevents Rpt3 tail docking into CP (2), thereby preventing Rpt3 docking into CP. At the end of assembly, CP outcompetes Nas6 for Rpt3, and the Rpt ring-CP interaction is formed (2). In my honors thesis, I investigate the mechanism and regulation of the competition between Nas6 and CP during proteasome assembly.

## Results and Discussion

***Rpt6 tail docking may promote CP competition for Rpt3 tail***

To test the competition between CP and Nas6 for Rpt3 tail, I used a disulfide crosslinking strategy, which was developed previously to define the registry between the hetero-hexameric Rpt ring and hetero-heptameric $\alpha$ ring (13). Specifically, Rpt3 tail docks into cognate $\alpha 2$ pocket. The last C-terminal amino acid in Rpt3 and the interacting (salt bridge) residue in $\alpha$ pocket have been substituted with cysteine residue, which are Rpt3-K428C and $\alpha$2-G79C, respectively. The yeast strain containing Rpt3-K428C and $\alpha$2-G79C

(Table 1) in their respective endogenous chromosomal loci was crossed to *nas6Δ* strain to compare Nas6's influence in the competition for Rp3 tail. The formation of disulfide bond between Rpt3-K428C and α2-G79C is achieved via a chemical crosslinker BMOE. It is important to note that only docking of a Rpt tail into an α pocket will allow formation of crosslink by BMOE. Crosslinked product can be readily detected due to combined molecular weight of crosslinked components, which will cause a shift in SDS-PAGE. Therefore, we are capturing endogenous Rpt-CP interaction. HA-tag was appended to the C-terminal end of α2 subunit to pull down proteasome and detect Rpt-α crosslink.

Under ADP and ATP condition, Rpt3-α2 crosslink (76 kDa) was comparable in the presence or absence of Nas6, indicating that CP prevails in competing for Rpt3 tail (Figure 1A). However, comparing between ATP condition and ADP condition, Rpt3-α2 crosslinking efficiency drastically decreased in ADP state (Figures 1A and 1D), indicating that nucleotides influenced Rpt3 tail docking. To confirm whether CP interaction with Rpt3 outcompetes Nas6, we checked the crosslinking between Rpt3 and noncognate α3 pocket, which has been shown to occur previously (13, 18). Similar to Rpt3-α2 crosslinking data (Figure 1a), difference was undetectable in Rpt3-CP crosslinking with and without Nas6. Crosslinking efficiency decreased again under ADP condition (Figures 1B and 1D). As expected, crosslinking signal of Rpt3-α3 was much weaker than cognate Rpt3-α2 (compare Figure 1A and 1B). The crosslinking data for Rpt3-α2 (Figure 1A) and Rpt3-α3 (Figure 1B) indicate that, regardless of nucleotide condition, the seemingly stronger CP attraction for Rpt3 tail masks Nas6's involvement in the competition.

What is exactly driving CP's competition towards Rpt3 against Nas6? To examine whether other CP-Rpt tail docking influences the competition between CP and Nas6 towards Rpt3, I performed disulfide crosslinking on Rpt3's dimer partner, Rpt6 (14-16). Rpt6 tail has demonstrated an exceptional specificity to α3 pocket and has been proposed to have an anchoring role during Rpt ring-CP assembly by guiding the docking of other Rpt tails on CP (13, 18). Under ATP and ADP condition, Rpt6-CP interaction readily formed regardless of Nas6 (Figure 1C). Curiously, the crosslinking efficiency was comparable between ATP and ADP, which indicates Rpt6-CP interaction is less nucleotide dependent compared to Rpt3-CP interaction (Figures 1C and 1D). Combined with Rpt3 crosslinking data (Figures 1A and 1B), the ability of Rpt6 tail to dock onto CP under any nucleotides appears to assist CP to continuously outcompetes Nas6 effect. In addition, as a Rpt dimer pair, the docking of Rpt6 may bring Rpt3 closer to CP, which is advantageous for CP interaction with Rpt3. This may explain why I could not capture Nas6 involvement in the competition for Rpt3 in any of the crosslinking data set. Even though Rpt6 tail drives the competition of CP towards Rpt3 tail, Rpt3 tail displays nucleotide dependence as evident from Rpt3 tail-CP crosslinking (Figures 1A and 1B). In summary, Rpt6 tail docking may promote CP's competition for Rpt3 tail.

***Rpt6 tail and Rpt3 tail jointly influence Nas6's competition against CP***

To examine the role of Nas6 in competing for Rpt3 tail, a single amino acid deletion was constructed in Rpt3 and Rpt6 C-terminus tail that is responsible for forming the salt bridge with corresponding $\alpha$ pocket, *rpt3Δ-1* and *rpt6Δ-1*, respectively. Under normal circumstances, Nas6 is absent from the proteasome holoenzyme but abnormally retains on the proteasome in *rpt3Δ-1* mutant (1, 2). Thus, the single amino acid deletion at Rpt3 C-terminus tail is predicted to relieve steric hindrance against Nas6 by exposing Rpt3's C-domain to Nas6. If my hypothesis that Rpt6 tail docking drives Nas6 competition towards Rpt3 tail is correct, then I should see an increase in Nas6 retention in *rpt3Δ-1 rpt6Δ-1* when Rpt6 tail docking is impaired.

Whole cell lysate of *rpt3-Δ1rpt6-Δ1* and corresponding singe mutants were resolved by 3.5% Native PAGE. The proteasomes holoenzymes ($RP_2$-CP and $RP_1$-CP) were then excised and resolved by SDS-PAGE. This strategy allows for detection of proteins present on the proteasome. The presence of Nas6 was vividly detected on *rpt3-Δ1rpt6-Δ1* proteasomes and only slightly on *rpt3-Δ1* or *rpt6-Δ1* proteasomes (Figure 2A). Apparent enrichment of Nas6 on *rpt3-Δ1rpt6-Δ1* proteasomes was not due to the level of proteasome, as indicated by the comparable level of lid (Rpn8) and base (Rpt5) (Figure 2A) nor the abundance of endogenous Nas6 (Figure 2C).Together with crosslinking data (Figure 1), the release of Nas6 from the RP-CP interface seems to be jointly regulated by Rpt6 and Rpt3 tail. In addition, the observation of slight Nas6 retention on *rpt6-Δ1* proteasomes may suggest that CP and Nas6 are competing equally for Rpt3 tail in *rpt6-Δ1* mutant when Rpt6 tail could not assist CP. Thus, Figure 2A provide some direct evidence for the critical role of Nas6 in competition for the Rpt3 tail.

Decreased activity of *rpt3-Δ1rpt6-Δ1* proteasomes suggests a defect in proteasome assembly as the RP-CP interface is compromised and suggests the importance of Rpt6-Rpt3 dimer. Since the level of the proteasome holoenzyme is relatively comparable between *rpt3-Δ1 rpt6-Δ1* and wild type, the fact that we see a greater retention, not like an additive effect, of Nas6 in double mutants suggests CP interaction of Rpt3 and Rpt6 tail are closely linked to each other. As expected, the amount of Nas6 was negligible on wild type proteasomes (Figure 2A).

Since proteasome activity decreased in *rpt3- Δ1rpt6- Δ1* cells (Figure 2B), the growth properties of *rpt3-Δ1rpt6-Δ1* were examined together with the turnover of ubiquitinated proteins, which directly reports any impairment in proteasome activity. Other Rpt dimers (Rpt4 with Rpt5 and Rpt1 and Rpt2) and their single counterparts were also included to study the importance of Rpt3-Rp6 dimer. Under normal growth condition at 30°C, all strains grew similarly with the exception of *rpt3-Δ1rpt6-Δ1* cells, which seemed to exhibit slight growth defect. This growth defect was drastically enhanced under heat stress at 37°C (Figure 2B). Together with the delayed turnover of ubiquitinated proteins at 30°C,

the decrease in cell viability is most likely due to impaired proteasome function.

The intimate link between Rpt6 and Rpt3 tail is also demonstrated by *rpt3-Δ1rpt6-Δ1* growth as it grew far worse than *rpt3-Δ1* or *rpt6-Δ1* under heat stress (Figure 2B). The slight growth defect observed for *rpt1-Δ1rpt2-Δ1* under 37$^{o}$C may be explained by the model where Rpt1 and Rpt2 dimer involves in later Rpt ring-CP interface formation compare Rpt6 and Rpt3 dimer (Figure 2D). In summary, the formation of proper RP-CP interface depends on Rpt6 tail and the competition between Nas6 and CP for Rpt3 tail.

***Potential response when Nas6 prevails in Rpt3 tail competition***

The data together illustrate proteasome formation when CP outcompetes Nas6 for Rpt3 tail binding. However, what could be the consequence when Nas6 prevails in Rpt3 binding and occludes CP, for example, in a state like Nas6-RP? Previous studies have suggested that the level of proteasomes declines in stationary phase, which shares many characteristics with the $G_0$ phase, correlating with decreased protein synthesis (19). Curiously, the level of RP chaperones remains constant, and it is a mystery as to why RP chaperones level is independent of proteasome level in stationary phase. Nas6 pulldown of stationary phase culture revealed visible RP and base bands (Figure 3A), and mass spectrometry of RP band not only revealed the presence of RP subunits but also another unexpected protein named Pim1. Pim1, a homolog of human LON protease, is an important protease in mitochondria (20). It is an ATP dependent protease and resides solely in mitochondria matrix. Pim1 degrades misfolded proteins that could not be refold and serve as the last step of protein quality control in mitochondria (21). Thus, Pim1's function is crucial in mitochondria in that it assists in maintaining protein homeostasis. Recently, Pim1 has been implicated in Parkinson's disease, where substrates of Pim1 were found at a abnormally high level (22). To verify the association of Nas6-RP with Pim1, we performed a reverse experiment where we pulled down through Pim1 side using TAP tag. Though Nas6 presence was observed (Figure 3B), we do not know if Nas6-RP association with Pim1 is directly or indirectly.

To examine the growth of Pim1, we performed spot assay with sever serial dilution under normal temperature 30$^{o}$C and mild temperature stress condition 34$^{o}$C. Since Pim1 is a mitochondrial protein, we also introduced mitochondrial stress through YPDR (0.1% dextrose, 2% raffinose) and YPR (2% raffinose) (24). Compare to dextrose, raffinose is a non-fermentable carbon source, which forces yeasts to utilize mitochondria to generate energy. Therefore, YPDR poses mild mitochondrial stress whereas YPR presents higher mitochondrial stress. To ensure the validity of my *pim1Δ* strain, clone A and B were included and both appeared to grow similar. Under YPD condition at 30$^{o}$, *pim1Δ* strain already exhibited severe growth defect compared to wild type and *nas6Δ* (Figure 3C). Under all the other conditions, *pim1Δ* seemed to display similar trend as other strains

(Figure 3C). However, in the presence of raffinose, there seems to be an alleviation of Pim1's growth defect (Figure 3C). The exact reason is still under investigation. *pim1Δnas6Δ* was not included in this assay as we observed heterogeneous population through dissection (Figure 3D, circled). Dissection of *pim1Δ* or *nas6Δ* displayed homogenous growth (data not shown). Since mitochondria is a double-membrane bound organelle that replicates and divides separately from the nucleus, *pim1Δnas6Δ* may affect the integrity of mitochondria division.

Pim1's association to Nas6-RP may be one of the response when Nas6-RP wins the competition for Rpt3 tail over CP. Therefore, these observations may suggest a potential link between two major degradation pathways: Pim1 in the mitochondria and proteasome in the nucleus and cytoplasm.

## Materials and Methods

### *Yeast Strain*

All the strains used in this research was in Sub62 (wild type) background. Please see table 1 for a complete list of strain mentioned in this project.

### *Antibodies*

Antibodies to Ubiquitin (BML-PW0930), Rpt5 (BML-PW8245), and Rpt3 (BML-PW8250) were purchased from Enzo Life Sciences. Antibodies to Rpt1 and Rpt6 and Rpn8, Rpn14, Nas6, Hsm3 were used. Pgk1 (459250, Invitrogen) was used as a loading control. HRP-conjugated anti-HA antibody (clone 3F10, 12013819001, Roche Life Science) was used to detect HA-tagged α2/α3.)

### *Phenotypic Assays*

Overnight yeast cultures were diluted into fresh YPD to $O.D._{600}$=0.2 and grown until $O.D._{600}$=0.8-1.2. Fresh cultures were diluted in sterile water to $O.D._{600}$=0.4 and series of consecutive 4-fold dilutions were made in 96-well plates. Cells were spotted onto fresh plates prepared 1 day before the experiments. Cells were grown for 2-3 days at indicated temperatures.

### *Preparation of Cell Lysate*

Yeast cells for exponential biochemical experiments were typically grown to $O.D._{600}$=3-5. For stationary phase experiments, yeast cells were grown for 8 days. Afterwards, culture was harvested by centrifugation at 3000 xg, washed with cold water, frozen and ground in the presence of liquid nitrogen as described previously (8, 24). Obtained cryo-lysates were hydrated with buffer, referred to as the proteasome buffer henceforth (50 mM Tris-HCl, pH 7.5, 5 mM $MgCl_2$, 1 mM EDTA, 10% glycerol, and protease inhibitors) that was supplemented with either 2 mM ATP and an ATP regeneration system or 2 mM ADP unless otherwise indicated. Hydrated cryo-lysates were centrifuged at 15,000 rpm for 30 min at 4°C to obtain whole cell lysates.

### *Consecutive Native PAGE, SDS-PAGE and Immunoblotting*

For consecutive native PAGE and SDS-PAGE assay, whole cell lysates were first resolved by 3.5% native PAGE, and subjected to an in-gel peptidase assay using LLVY-AMC (Suc-Leu-Leu-Val-Tyr-AMC, 4011369, Bachem) in a buffer (50 mM Tris-HCl, pH 7.5, 5 mM $MgCl_2$, 1 mM ATP, 10 M LLVY-AMC) for 15 min at 30°C. The proteasomes were then visualized under UV light, and excised horizontally as a strip. Native gel strips were soaked in 1x SDS Laemmli sample buffer for 15 min at room temperature and subjected to 12% SDS-PAGE as described previously (12, 25).

### *Crosslinking*

All strains used for crosslinking experiments carry a 3xHA tag that was appended to the C-terminus of the indicated α subunit in their endogenous chromosomal loci (Supplementary table s1). The crosslinking procedure was essentially performed as described previously(13). Cell lysates were equalized to 600 μl (approximately 2.5 mg of total cell protein) in the proteasome buffer and incubated with 10 μl of HA-agarose beads (Anti-HA Affinity Matrix, 11815016001, Roche Life Science) on the rotator in 4ºC for 1.5 hr. HA-resin-bound proteasomes were then precipitated by centrifugation at 15,000 rpm for 30 s at 4ºC, and were washed twice with 400 μl of wash buffer (50 mM Tris-HCl, pH 7.5, 5 mM $MgCl_2$, 1 mM EDTA, 10% glycerol, 150 mM NaCl) supplemented with 1 mM ATP or 0.5 mM ADP at 4ºC. HA-resin-bound proteasomes were resuspended in 50 μl proteasome buffer and divided into two tubes, which were incubated with a chemical crosslinker, BMOE (Bis-Maleimidoethane, 22323, Thermo Scientific) at 0.1 mM, or a solvent, DMF (D4551, Sigma-Aldrich) for 1 hr on the rotator at 4ºC. Crosslinking was quenched by boiling at 95ºC in 55 μl Laemmli 1x sample buffer with 2.5% β-ME and resolved by 12% SDS-PAGE and immunoblotting.

### *Complex Purification*

Yeasts cultures were grown to stationary phase and cells were harvested by centrifugation, frozen and ground in the presence of liquid nitrogen. Nas6 complex were affinity-purified via Flag tag using flag resin following procedures described previously (26). Pim1 complex were affinity-purified via Pim1-TeV-ProA tag using IgG resin (0855961, MP Biomedicals) following the procedures described previously (26) except one modification that all buffers contained 10% glycerol throughout the purification. Pim1 complexes were eluted from IgG resin using TEV protease (V6101, ProTEV Promega).

### *Yeast Tetrad Dissection*

*pim1Δ* was crossed with nas6Δ following procedure described previously (28).

**Acknowledgments**

I would like to thank my thesis advisor, Dr. Soyeon Park, for developing my critical thinking and inquisitive skills. In addition, I am grateful for her patience, tolerance, and guidance for allowing me to complete my honors thesis project. I would like to thank Dr. Vladyslava Sokolova for her mentorship and support. I would like to thank the members of my thesis committee Drs. Sabrina Spencer, Jennifer Martin, and Christy Fillman.

**References**

1. Park, S., Roelofs, J., Kim, W., Robert, J., Schmidt, M., Gygi, S. P., and Finley, D. (2009) Hexameric assembly of the proteasomal ATPases is templated through their C termini. *Nature* **459**, 866-870
2. Roelofs, J., Park, S., Haas, W., Tian, G., McAllister, F. E., Huo, Y., Lee, B. H., Zhang, F., Shi, Y., Gygi, S. P., and Finley, D. (2009) Chaperone-mediated pathway of proteasome regulatory particle assembly. *Nature* **459**, 861-865
3. Satoh, T., Saeki, Y., Hiromoto, T., Wang, Y. H., Uekusa, Y., Yagi, H., Yoshihara, H., Yagi-Utsumi, M., Mizushima, T., Tanaka, K., and Kato, K. (2014) Structural basis for proteasome formation controlled by an assembly chaperone nas2. *Structure* **22**, 731-743
4. Kish-Trier, E., and Hill, C. P. (2013) Structural biology of the proteasome. *Annual review of biophysics* **42**, 29-49
5. Finley, D. (2009) Recognition and processing of ubiquitin-protein conjugates by the proteasome. *Annual review of biochemistry* **78**, 477-513
6. Ciechanover, A., and Brundin, P. (2003) The ubiquitin proteasome system in neurodegenerative diseases: sometimes the chicken, sometimes the egg. *Neuron* **40**, 427-446
7. Matyskiela, M. E., Lander, G. C., and Martin, A. (2013) Conformational switching of the 26S proteasome enables substrate degradation. *Nat Struct Mol Biol* **20**, 781-788
8. Smith, D. M., Chang, S. C., Park, S., Finley, D., Cheng, Y., and Goldberg, A. L. (2007) Docking of the proteasomal ATPases' carboxyl termini in the 20S proteasome's alpha ring opens the gate for substrate entry. *Mol Cell* **27**, 731-744
9. Lander, G. C., Estrin, E., Matyskiela, M. E., Bashore, C., Nogales, E., and Martin, A. (2012) Complete subunit architecture of the proteasome regulatory particle. *Nature* **482**, 186-191
10. Vilchez, D., Boyer, L., Morantte, I., Lutz, M., Merkwirth, C., Joyce, D., Spencer, B., Page, L., Masliah, E., Berggren, W.T., et al. (2012). Increased proteasome activity in human embryonic stem cells is regulated by PSMD11. Nature **489**, 304–308.

11. Kruegel, U., Robison, B., Dange, T., Kahlert, G., Delaney, J.R., Kotireddy, S., Tsuchiya, M., Tsuchiyama, S., Murakami, C.J., Schleit, J., et al. (2011). Elevated Proteasome Capacity Extends Replicative Lifespan in Saccharomyces cerevisiae. PLoS Genetics **7**, e1002253.
12. Tomko, R. J., Jr., Funakoshi, M., Schneider, K., Wang, J., and Hochstrasser, M. (2010) Heterohexameric ring arrangement of the eukaryotic proteasomal ATPases: implications for proteasome structure and assembly. *Mol Cell* **38**, 393-403
13. Tian, G., Park, S., Lee, M. J., Huck, B., McAllister, F., Hill, C. P., Gygi, S. P., and Finley, D. (2011) An asymmetric interface between the regulatory and core particles of the proteasome. *Nat Struct Mol Biol* **18**, 1259-1267
14. Funakoshi, M., Tomko, R. J., Jr., Kobayashi, H., and Hochstrasser, M. (2009) Multiple assembly chaperones govern biogenesis of the proteasome regulatory particle base. *Cell* **137**, 887-899
15. Kaneko, T., Hamazaki, J., Iemura, S., Sasaki, K., Furuyama, K., Natsume, T., Tanaka, K., and Murata, S. (2009) Assembly pathway of the Mammalian proteasome base subcomplex is mediated by multiple specific chaperones. *Cell* **137**, 914-925
16. Saeki, Y., Toh, E. A., Kudo, T., Kawamura, H., and Tanaka, K. (2009) Multiple proteasome-interacting proteins assist the assembly of the yeast 19S regulatory particle. *Cell* **137**, 900-913
17. Le Tallec, B., Barrault, M. B., Guerois, R., Carre, T., and Peyroche, A. (2009) Hsm3/S5b participates in the assembly pathway of the 19S regulatory particle of the proteasome. *Mol Cell* **33**, 389-399
18. Park, S., Li, X., Kim, H. M., Singh, C. R., Tian, G., Hoyt, M. A., Lovell, S., Battaile, K. P., Zolkiewski, M., Coffino, P., Roelofs, J., Cheng, Y., and Finley, D. (2013) Reconfiguration of the proteasome during chaperone-mediated assembly. *Nature* **497**, 512-516
19. Bajorek, M., Finley, D., and Glickman, M.H. (2003). Proteasome disassembly and downregulation is correlated with viability during stationary phase. Current Biology **13,** 1140–1144.
20. Ngo, J.K., Pomatto, L.C.D., and Davies, K.J.A. (2013). Upregulation of the mitochondrial Lon Protease allows adaptation to acute oxidative stress but dysregulation is associated with chronic stress, disease, and aging. Redox Biology **1**, 258–264.
21. Bender, T., Lewrenz, I., Franken, S., Baitzel, C., and Voos, W. (2011). Mitochondrial enzymes are protected from stress-induced aggregation by mitochondrial chaperones and the Pim1/LON protease. Molecular Biology of the Cell **22,** 541–554.

22. Pickrell, A.M., and Youle, R.J. (2015). The Roles of PINK1, Parkin, and Mitochondrial Fidelity in Parkinson's Disease. Neuron ***85***, 257–273.
23. Erjavec, N., Bayot, A., Gareil, M., Camougrand, N., Nystrom, T., Friguet, B., and Bulteau, A.-L. (2013). Deletion of the mitochondrial Pim1/Lon protease in yeast results in accelerated aging and impairment of the proteasome. Free Radical Biology and Medicine ***56***, 9–16.
24. Gillette, T. G., Kumar, B., Thompson, D., Slaughter, C. A., and Demartino, G. N. (2008) Differential roles of the C-termini of AAA subunits of PA700 (19S regulator) in asymmetric assembly and activation of the 26s proteasome. *J Biol Chem* **283**, 31813-31822
25. Park, S., Kim, W., Tian, G., Gygi, S. P., and Finley, D. (2011) Structural defects in the regulatory particle-core particle interface of the proteasome induce a novel proteasome stress response. *J Biol Chem* **286**, 36652-36666
26. Leggett, D. S., Glickman, M. H., and Finley, D. (2005) Purification of proteasomes, proteasome subcomplexes, and proteasome-associated proteins from budding yeast. *Methods in Molecular Biology* **301**, 57-70
27. Finley, D., Ozkaynak, E., and Varshavsky, A. (1987) The yeast polyubiquitin gene is essential for resistance to high temperatures, starvation, and other stresses. *Cell* **48**, 1035-1046
28. Morin, A., Moores, A.W., and Sacher, M. (2009). Dissection of Saccharomyces Cerevisiae Asci. Journal of Visualized Experiments.

## Figure Legends

***Figure 1. Rpt6 tail may assist in CP's competition for Rpt3 tail binding.***

(*A*) Crosslinking strategy was performed on wild type or *nas6D* harboring a cognate crosslinking pair (Rpt3-K428C and α2-A79C) in their respective chromosomal loci. Proteasomes were immunoprecipitated with 3xHA tag at the C-terminus of α2 subunit using HA beads. The beads-bound proteasomes were then crosslinked with BMOE, or incubated with its solvent, DMF at 0.1mM final concentration as a control for 1.5 hr on ice, and quenched by boiling in Laemmli sample buffer and resolved by 12% SDS-PAGE. Rpt-α crosslinks were detected by immunoblotting with antibodies for Rpt3 (top) and HA epitope (bottom). Molecular weight markers are at left in kDa. Asterisk (*) is a non-specific signal in crosslinking under ADP conditions. Note the Asterisks in (B) and (C) in ADP.

(*B*) Crosslinking experiments were conducted as described in (A) for noncognate pair, Rpt3-K428C and α3-T81C in wild-type or *nas6Δ* strains.

(*C*) Crosslinking experiments were conducted on wild type or *nas6D* harboring a cognate Rpt6-K405C and α3-T81C.

(*D*) Graphical representation of the crosslinks formation of cognate Rpt3-α2 pair (A) and Rpt6-α3 pair (C). Image J software was used to quantify crosslinking efficiency of [Rpt-α crosslinked bands]/[Rpt bands + Rpt-α crosslinked bands], which are marked by arrows individually in (A) and (C). For this, we used the signal intensities for Rpt subunits, which appear sharper than α subunits to obtain reliable measurements. Non-cognate Rpt3-α3 crosslinks (B) in ADP generate very weak signals, which are not suitable for quantification.

***Figure 2. Rpt6 tail and Rpt3 tail jointly influence Nas6's competition against CP.***

(*A*) Whole cell lysates (40 μg) from indicated strains were first resolved by 3.5% native gel. Following the in-gel peptidase assay using LLVY-AMC, the native gel region containing proteasome holoenzymes ($RP_2$-CP and $RP_1$-CP) was excised horizontally as a strip and directly loaded onto 12% SDS-PAGE to further resolve the components of the proteasomes on the native gel piece. Immunoblotting was performed for indicated proteins. Rpn8, a lid subunit and Rpt5, a base subunit serve as loading controls for proteasome amounts in the native gel strip.

(*B*) Growth phenotypes of the indicated strains were assessed via 4-fold serial dilution. Strains were spotted on the YPD plates and grown for 2-3 days at 30°C and 37°C.

(*C*) Whole cell lysates (20 μg) were resolved by 10% Bis-Tris SDS-PAGE (detection for ubiquitinated protein), or 12% Tris-Glycine SDS-PAGE and analyzed by immunoblotting for indicated proteins. Rpn8 is a lid subunit. Rpt3 and Rpt6 are base subunits. Pgk1 is a loading control.

(*D*) A model for RP-CP assembly. At the early stage of Rpt ring assembly, Rpt6 tail anchors onto the CP promote the joining of the Rpt2-Rpt1 module (18) depicted in left. Nas6

antagonizes Rpt3 tail docking into the CP and delays the joining of the Rpt4-Rpt5 module (18). At the mature proteasome holoenzyme, Rpt3 tail docks into the CP in the proteasome holoenzyme and mediate CP gate opening via its C-terminal HbYX motif as depicted at right side of the model. Only the outermost a ring was depicted in the CP. Three other RP chaperones, Rpn14, Hsm3 and Nas2 were omitted.

***Figure 3. Potential implication when Nas6 prevails in Rpt3 tail binding***

(*A*) Nas6 complexes were affinity-purified in stationary phase via an affinity tag Flag on Nas6 and (80 μg) was resolved onto Native PAGE. The gel was then stained with Coomassie Brilliant Blue to visualize purified Na6 complexes. RP and base bands were observed and mass spectrometry of RP bend indicates Pim1's presence.

(*B*) Pim1 complexes were affinity-purified in stationary phase via an affinity tag TeV-ProA and 20 μg resolved by 12% Tris-Glycine SDS-PAGE and analyzed by immunoblotting for presence of Nas6. Rpn5 and Rp8, lid subunits and Rpt5, a base subunit serve as loading controls.

(*C*) Growth phenotypes of the indicated strains were assessed via 7-fold serial dilution. Strains were spotted on YPD plates to mimic no mitochondrial stress, YPDR plates to mild mitochondrial stress, and YPR plates to severe mitochondrial stress and grown for 2-4 days at the indicated temperature.

(*D*) Dissection plate of *nas6Δ* crossed with *pim1Δ*. Spores circled in red indicate *nas6Δpim1Δ* genotype.

**Table 1. List of strains mentioned in the study**

| Strain | Relevant Genotype | Figures | Reference |
|---|---|---|---|
| SUB62 | *MAT**a**, lys2-801, leu2-3, 2-112, ura3-52, his3-Δ200, trp1-1* | 2, 3 | (27) |
| SP1729A | *MAT**a**, rpt6::rpt6-Δ1(kanMX6)* | 2 | This study |
| SP1477A | *MAT**a**, rpt3::rpt3-Δ1(kanMX6)* | 2 | This study |
| SP1785A | *MAT**a**, rpt3::rpt3-Δ1(kanMX6), rpt6::rpt6-Δ1(kanMX6)* | 2 | This study |
| SP1781A | *MATα, rpt3::rpt3-Δ1(kanMX6)* | 2 | This study |
| SP1694A | *MATα, nas6::TRP1* | 3 | This study |
| SP1677 | *MAT**a** , nas6::Nas6-3Flag (hyg)* | 3 | This study |
| SP2200 | *MAT**a** , pim1::URA3* | 3 | This study |
| SP2273 | *MAT**a** , pim1::kanMX6* | 3 | This study |

| | | | |
|---|---|---|---|
| SP2274 | *MAT**a** , pim1:: hyg* | 3 | This study |
| SP2198 | *MAT**a** , pim1::Pim1-TAP (HIS3)* | 3 | This study |
| SP2199 | *MATα , pim1::Pim1-TAP (HIS3), nas6::TRP1* | 3 | This study |
| SP2201 | *MATα , pim1::URA3, nas6::TRP1* | 3 | This study |
| SP2278 | *MATα , pim1::kanMX6, nas6::TRP1* | 3 | This study |
| SP2279 | *MATα , pim1:: hyg, nas6::TRP1* | 3 | This study |
| SP1863A | *MATα, rpt6::rpt6-K405C(kanMX6), α3::α3-T81C-3HA(TRP1)* | 1 | This study and (13) |
| SP1864A | *MAT**a**, rpt6::rpt6-K405C(kanMX6), α3::α3-T81C-3HA(TRP1), nas6::TRP1* | 1 | This study and (13) |
| SP1879A | *MAT**a**, rpt3::rpt3-K428C(kanMX6), α3::α3-T81C-3HA(TRP1)* | 1 | This study and (13) |
| SP1995A | *MAT**a**, rpt3::rpt3-K428C(kanMX6), α3::α3-T81C-3HA(TRP1), nas6::TRP1* | 1 | This study and (13) |
| SP2000A | *MAT**a**, rpt3::rpt3-K428C(kanMX6), α2::α2-G79C-3HA(TRP1), nas6::TRP1* | 1 | This study and (13) |
| SP2001B | *MATα, rpt3::rpt3-K428C(kanMX6), α2::α2-G79C-3HA(TRP1)* | 1 | This study and (13) |

All strains are congenic to SUB62 and carry the lys2-801, leu2-3, 2-112, ura3-52, his3-Δ200, trp1-1 markers. We refer to α subunit genes using standard proteasome nomenclature. The standard yeast gene names are as follows: α2 by PRE8, α3 by PRE9

Figure 1.

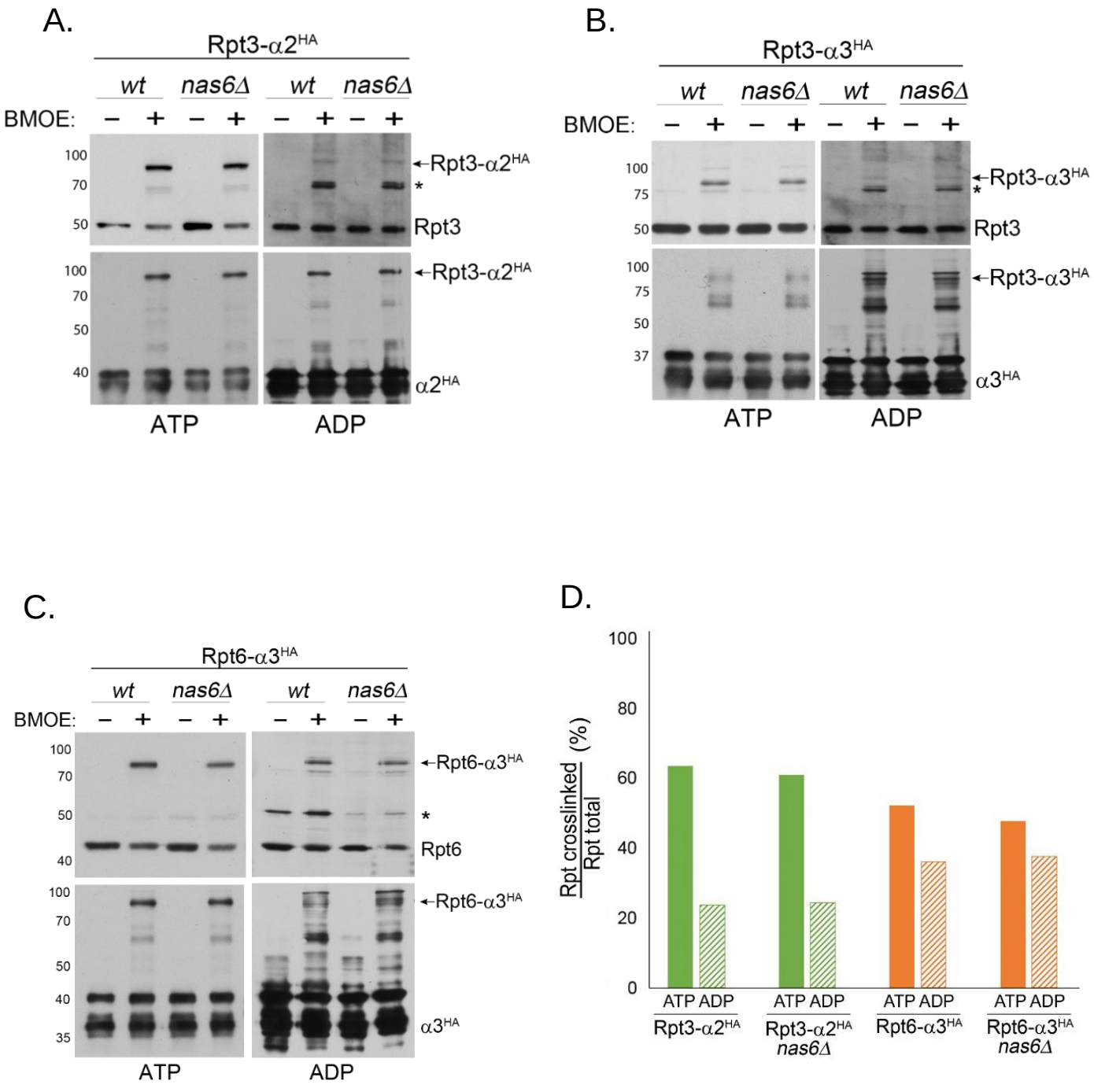
A.
Rpt3-α2HA
wt
nas6Δ
wt
nas6Δ
BMOE:
– + – + – + – +
100
70
50
40
←Rpt3-α2HA
*
Rpt3
←Rpt3-α2HA
α2HA
ATP
ADP
B.
Rpt3-α3HA
wt
nas6Δ
wt
nas6Δ
BMOE:
– + – + – + – +
100
75
50
37
←Rpt3-α3HA
*
Rpt3
←Rpt3-α3HA
α3HA
ATP
ADP
C.
Rpt6-α3HA
wt
nas6Δ
wt
nas6Δ
BMOE:
– + – + – + – +
100
70
50
40
35
←Rpt6-α3HA
*
Rpt6
←Rpt6-α3HA
α3HA
ATP
ADP
D.
Rpt crosslinked / Rpt total (%)
100
80
60
40
20
0
ATP ADP
Rpt3-α2HA
ATP ADP
Rpt3-α2HA nas6Δ
ATP ADP
Rpt6-α3HA
ATP ADP
Rpt6-α3HA nas6Δ

Figure 2.

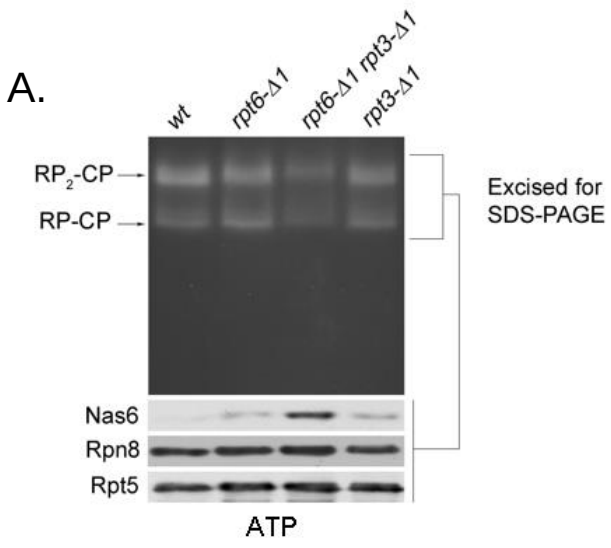
A.
wt
rpt6-Δ1
rpt6-Δ1 rpt3-Δ1
rpt3-Δ1
RP2-CP
RP-CP
Excised for SDS-PAGE
Nas6
Rpn8
Rpt5
ATP

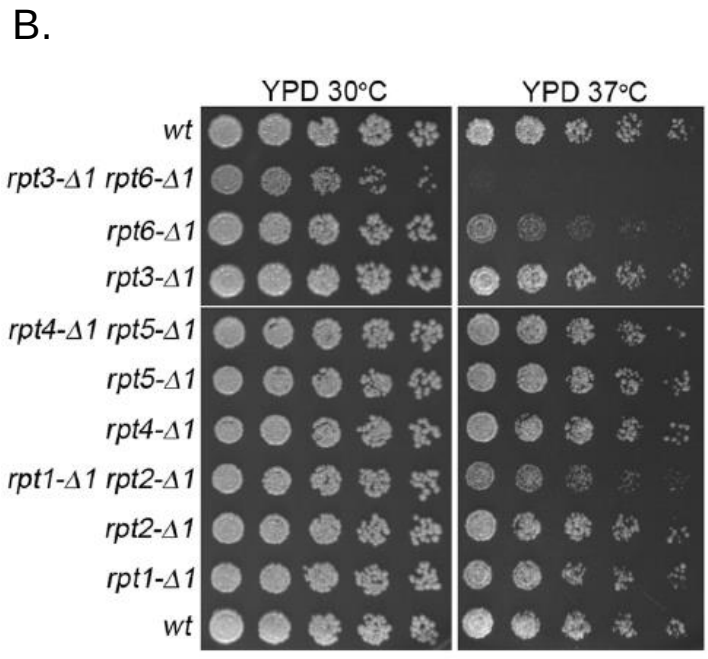
B.
YPD 30°C
YPD 37°C
wt
rpt3-Δ1 rpt6-Δ1
rpt6-Δ1
rpt3-Δ1
rpt4-Δ1 rpt5-Δ1
rpt5-Δ1
rpt4-Δ1
rpt1-Δ1 rpt2-Δ1
rpt2-Δ1
rpt1-Δ1
wt

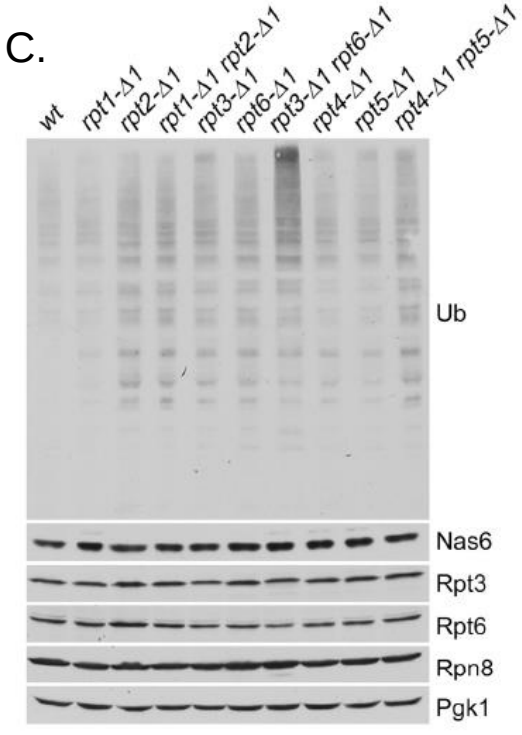
C.
wt
rpt1-Δ1
rpt2-Δ1
rpt1-Δ1 rpt2-Δ1
rpt3-Δ1
rpt6-Δ1
rpt3-Δ1 rpt6-Δ1
rpt4-Δ1
rpt5-Δ1
rpt4-Δ1 rpt5-Δ1
Ub
Nas6
Rpt3
Rpt6
Rpn8
Pgk1

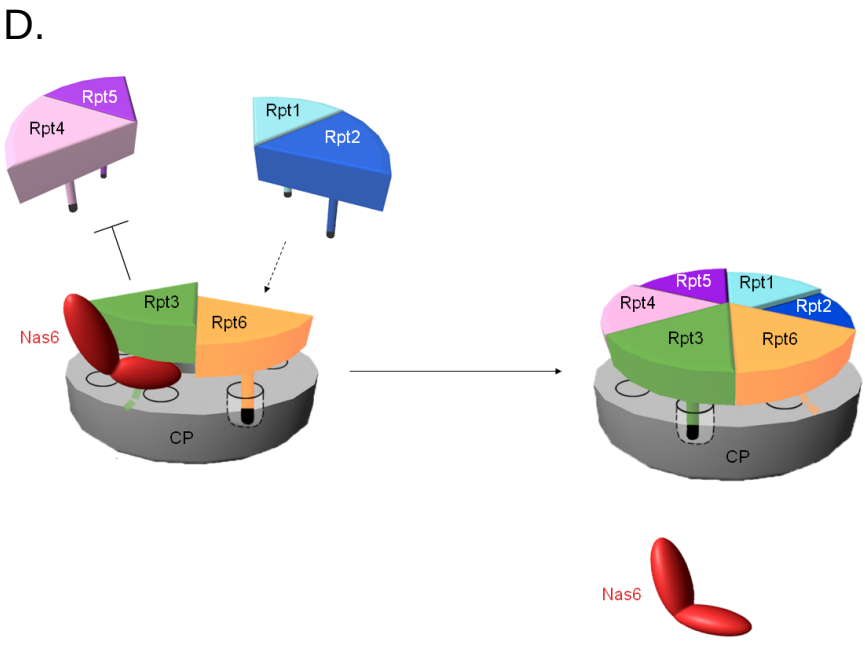
D.
Rpt5
Rpt4
Rpt1
Rpt2
Nas6
Rpt3
Rpt6
CP
Rpt5
Rpt1
Rpt4
Rpt2
Rpt3
Rpt6
CP
Nas6

Figure 3.

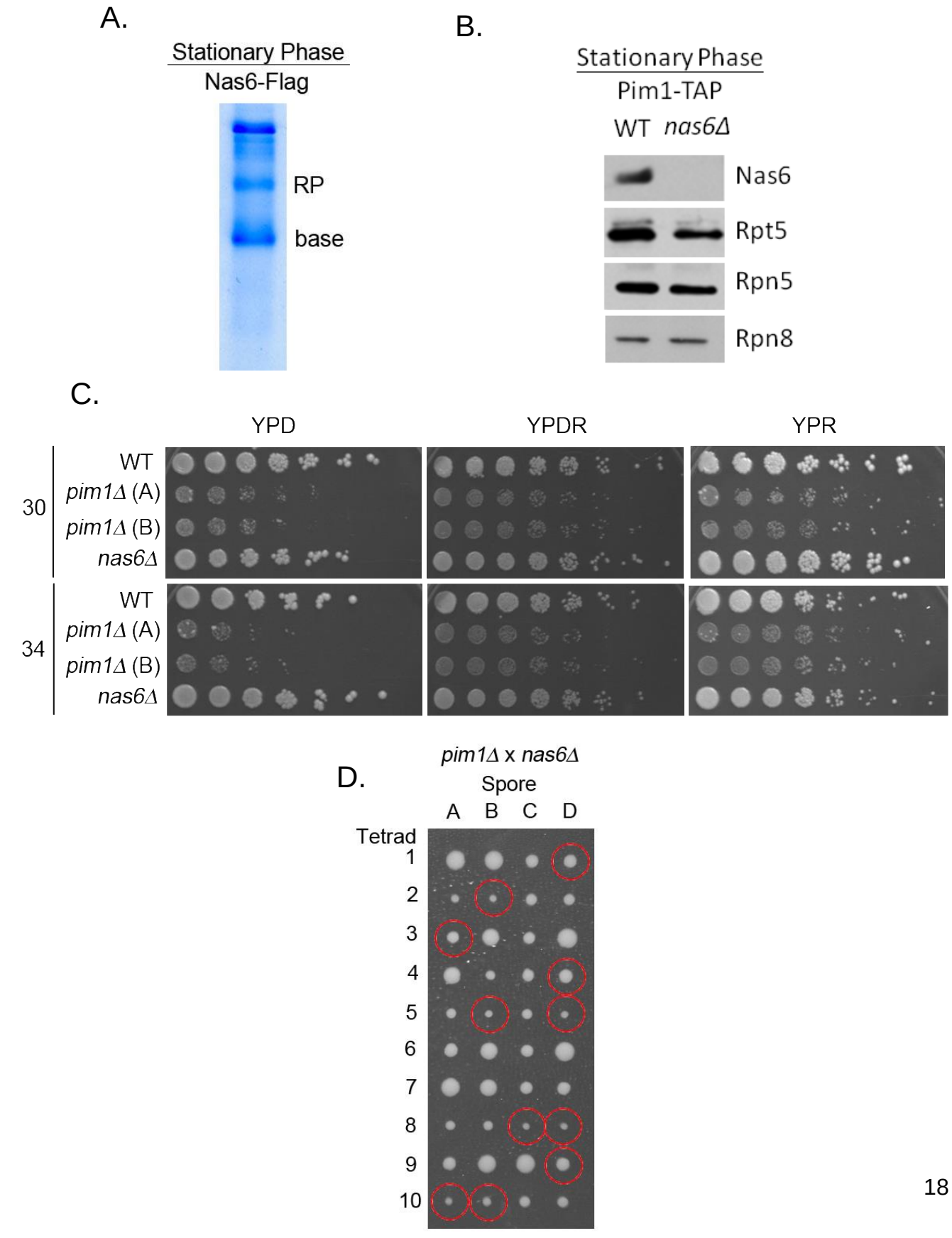
A.
Stationary Phase
Nas6-Flag
RP
base
B.
Stationary Phase
Pim1-TAP
WT nas6Δ
Nas6
Rpt5
Rpn5
Rpn8
C.
YPD
YPDR
YPR
30
34
WT
pim1Δ (A)
pim1Δ (B)
nas6Δ
D.
pim1Δ x nas6Δ
Spore
A B C D
Tetrad
1
2
3
4
5
6
7
8
9
10